Electroweak physics in the forward region

Marek Sirendi* on behalf of the LHCb collaboration
* University of Cambridge, sirendi@hep.phy.cam.ac.uk

1 Motivation

Precision measurements of $\sigma_{W(Z)}$ are important tests of perturbative QCD and EWK theory.

The factorisation theorem gives the pp $\rightarrow$ X cross section, σ, in terms of the partonic cross section, $\hat{\sigma}$, as

$$\sigma_{pp\rightarrow X} = \sum_{a,b} \int dx_a\, dx_b\, f_a(x_a, Q^2)\, f_b(x_b, Q^2)\, \hat{\sigma}_{ab\rightarrow X}(Q^2),$$

where f_i are parton distribution functions (PDF) evaluated at momentum fraction x and momentum transfer squared Q^2.

$\hat{\sigma}_{W(Z)}$ is known to high precision: NNLO in QCD and NLO in EWK theory with an accuracy of $<1\%$. Therefore, these measurements act as "standard candles" that can be used to probe PDFs.

While ATLAS/CMS is mostly limited to a pseudorapidity of $\eta \leq 2.5$ (with Bjorken-x in the range of $10^{-3} \leq x \leq 0.1$), LHCb detects W and Z daughters in $2 < \eta < 5$, where $\eta = -\ln\left[\tan\left(\frac{\theta}{2}\right)\right]$. These are formed in a highly boosted system with respect to the lab frame with one parton at $x_a \sim 0.1$ and the other at $x_b \sim 10^{-4}$.

$$y_{W(Z)} = \ln\left(\frac{x_a}{x_b}\right)^{\frac{1}{2}} \Longrightarrow x_{a,b} = \frac{M_{W(Z)}}{\sqrt{s}} e^{\pm y_{W(Z)}}$$

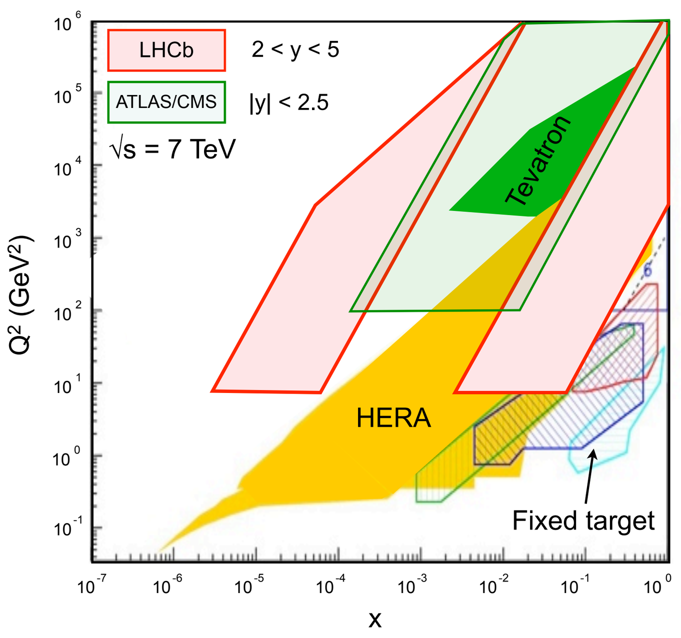

LHCb acceptance in $x-Q^2$ phase space. LHCb probes a unique region of phase space at low x and high Q^2.

2 Impact on PDFs

PDF uncertainties become particularly large at forward boson rapidities making LHCb uniquely placed to contribute.

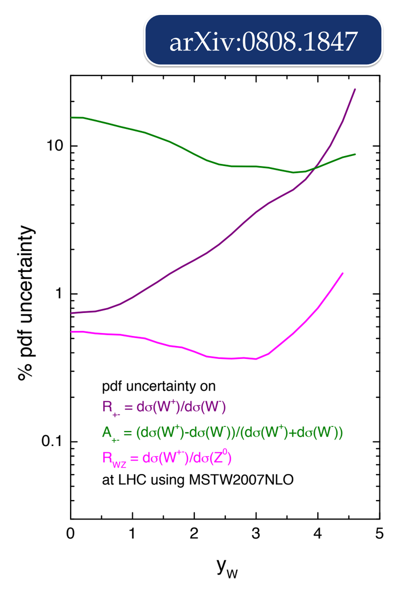

PDF uncertainty as a function of y_W for ratio measurements R_{W^+/W^-} and $R_{W/Z}$, and the charge asymmetry.

The charge asymmetry is defined as

$$\mathcal{A}(\eta_\ell) \equiv \frac{\frac{d\sigma^{W^+}}{d\eta_\ell} - \frac{d\sigma^{W^-}}{d\eta_\ell}}{\frac{d\sigma^{W^+}}{d\eta_\ell} + \frac{d\sigma^{W^-}}{d\eta_\ell}} \approx \frac{u - d}{u + d} \approx \frac{u_{val} - d_{val}}{u_{val} + d_{val} + 2u_{sea}}.$$

LHCb data of W production provide the largest impact on valence d and sea light quark PDFs due to the forward kinematics probed by the experiment.

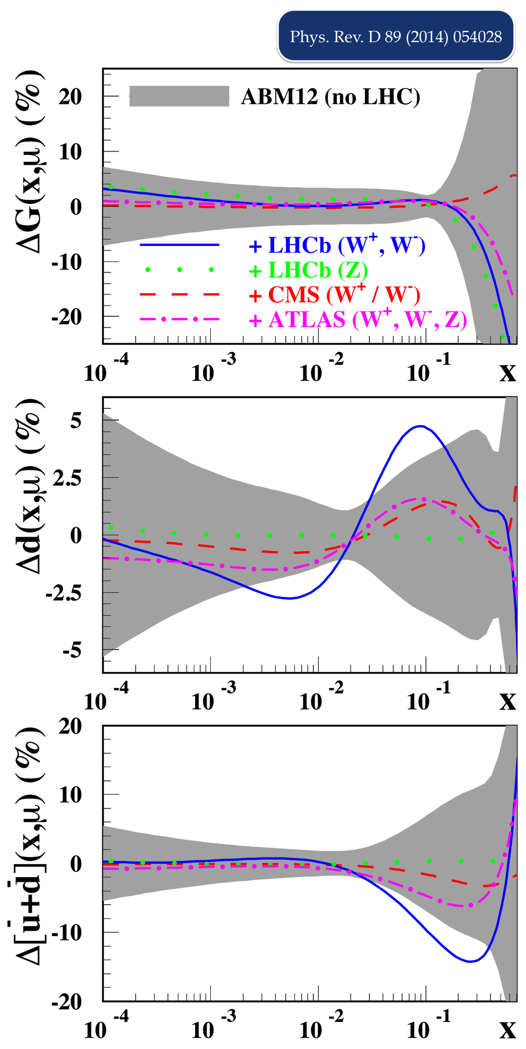

The 1σ band for the 4-flavour NNLO ABM12 PDFs versus x (shaded area) with the relative difference to the PDF from the inclusion of various LHC electroweak measurements.

3 W cross-section

The W cross-section is measured in the muon final state with $p_T^\mu > 20$ GeV and $2.0 < \eta^\mu < 4.5$.

The signature for W production is a single high-p_T isolated muon, however, significant backgrounds remain from Z $\rightarrow \mu\mu$ and decay in flight, $K/\pi \rightarrow \mu\nu$. The analysis strategy is to fit p_T^μ for the signal yield. Signal and electroweak templates are taken from simulation and the decay in flight component floats freely in the fit with a template determined from data.

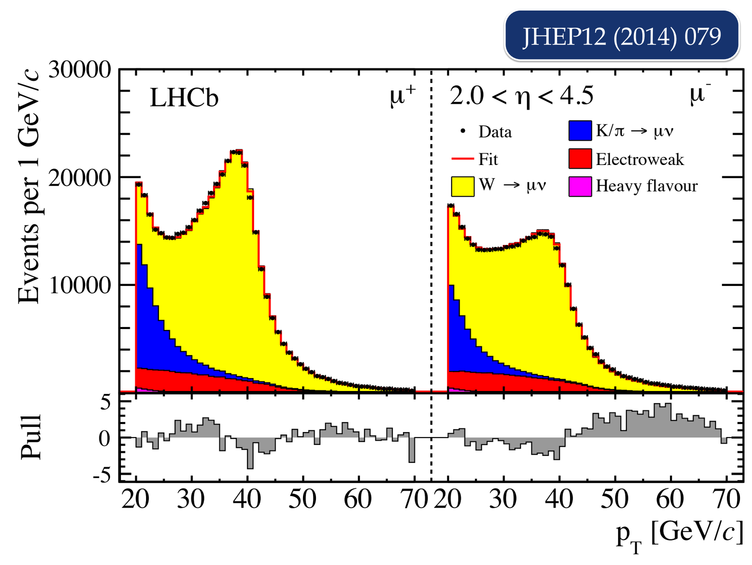

p_T^μ distribution for μ^+ (left) and μ^- (right) fitted for signal and backgrounds. Pull distributions are shown underneath.

$\sigma_{W\rightarrow\mu\nu}$ cross-section at 7 TeV is measured to be

$$\sigma_{W^+\rightarrow\mu^+\nu} = 861.0 \pm 2.0\,(stat.) \pm 11.2\,(syst.) \pm 14.7\,(lumi.)\text{pb}$$

$$\sigma_{W^-\rightarrow\mu^-\nu} = 675.8 \pm 1.9\,(stat.) \pm 8.8\,(syst.) \pm 11.6\,(lumi.)\text{pb}$$

The cross-section ratio is measured to be

$$\frac{\sigma_{W^+\rightarrow\mu^+\nu}}{\sigma_{W^-\rightarrow\mu^-\nu}} = 1.274 \pm 0.005\,(stat.) \pm 0.009\,(syst.)$$

Results are corrected for FSR and contrasted to a NNLO calculation from FEWZ along with a selection of NNLO PDF sets.

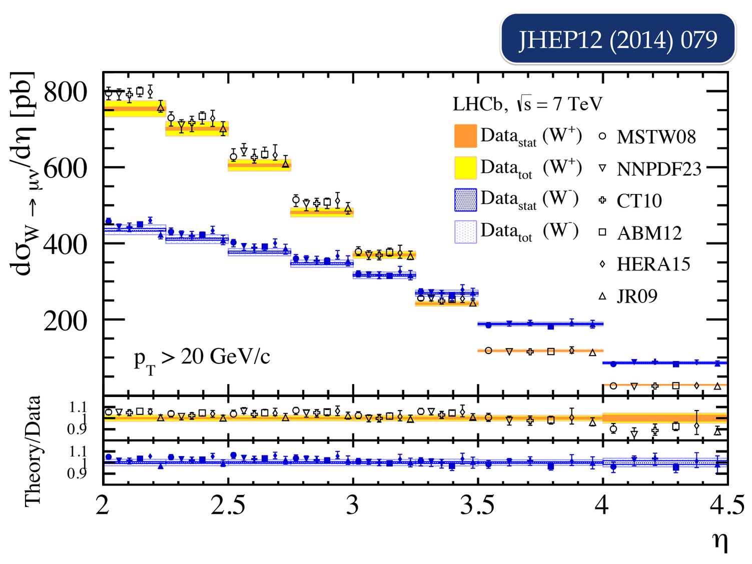

Differential σ_W in bins of η_μ. The inner bands correspond to the statistical uncertainty and the outer bands to the total uncertainty. NNLO predictions are superimposed.

4 W charge asymmetry

The charge asymmetry is also measured. $\mathcal{A}(\eta_\ell)$ is almost completely insensitive to higher order QCD corrections and several experimental uncertainties also cancel. Therefore, a measurement of this quantity is a powerful probe of PDFs.

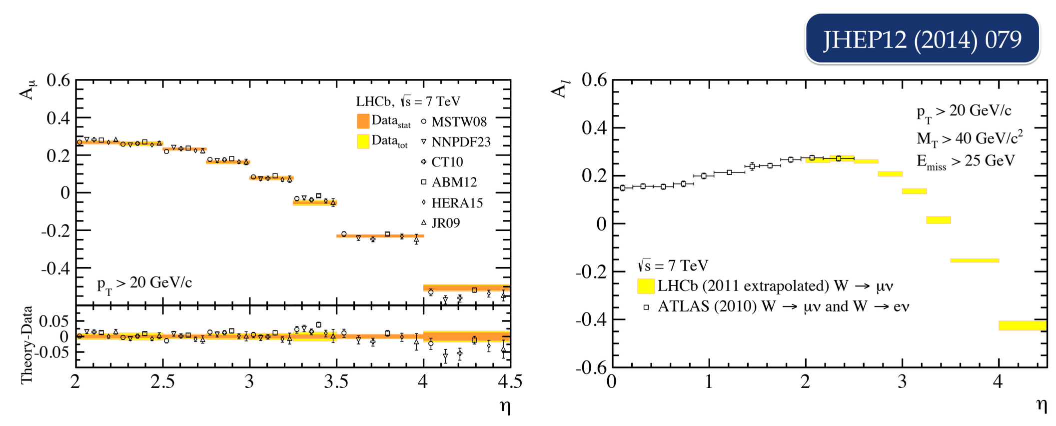

The lepton charge asymmetry in LHCb acceptance (left) and extrapolated to the fiducial volume of ATLAS (right). The LHCb measurement is seen to be complementary to that of ATLAS.

5 Z cross-section

The Z cross-section is measured in the electron final state with $p_T^e > 20$ GeV, $2.0 < \eta^e < 4.5$, and $60 < M_{ee} < 120$ GeV.

$\sigma_{Z\rightarrow e^+e^-}$ cross-section at 8 TeV is measured to be

$$\sigma_{Z\rightarrow e^+e^-} = 93.81 \pm 0.41\,(stat.) \pm 1.48\,(syst.) \pm 1.14\,(lumi.)\text{pb}$$

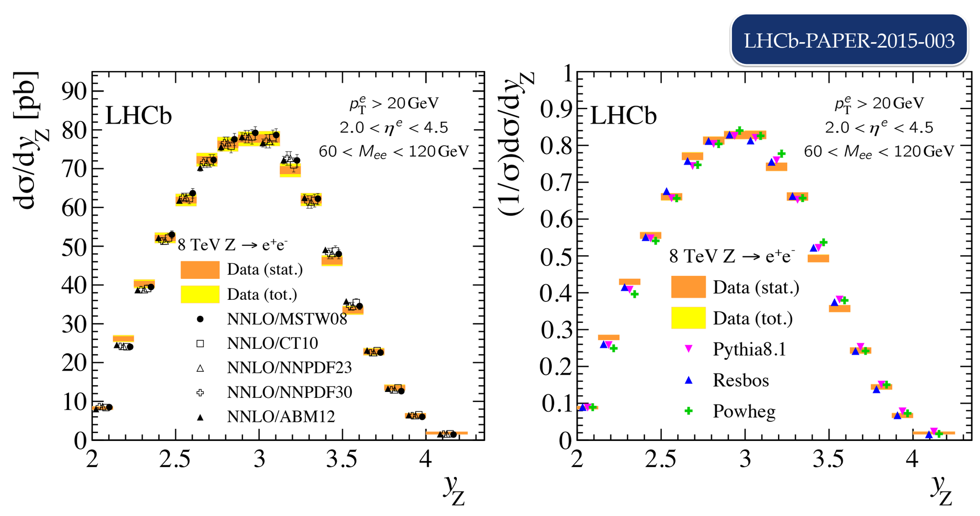

Differential σ_Z in bins of y_Z. The inner bands correspond to the statistical uncertainty and the outer bands to the total uncertainty. NNLO (left) and generator (right) predictions are superimposed. The right-hand side plot has been normalised by the total cross-section.

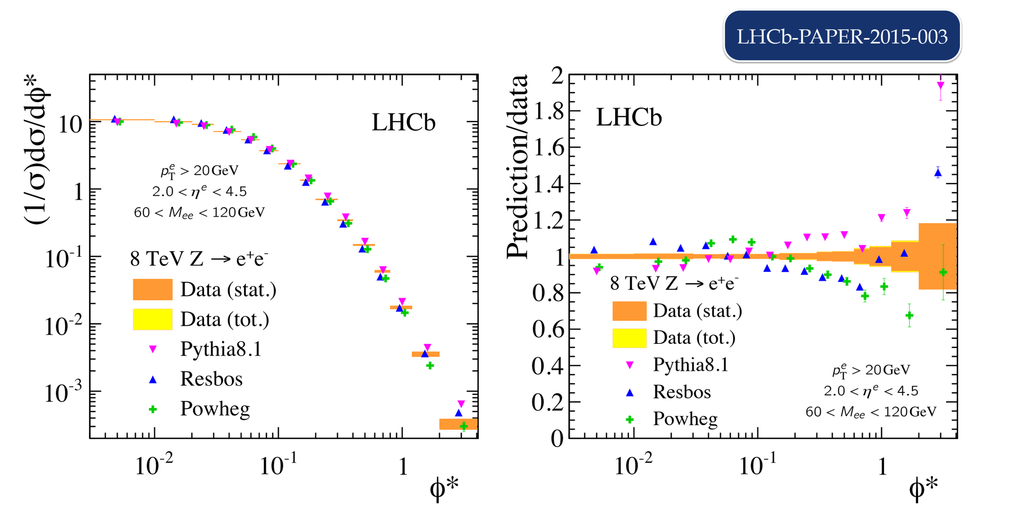

Normalised differential σ_Z in bins of ϕ^* (top) and the ratio of prediction to data (bottom).

$$\phi^* \equiv \tan(\phi_{acop}/2)/\cosh(\Delta\eta/2) \approx p_T/M,$$

where $\phi_{acop} \equiv \pi - |\Delta\phi|$, $\Delta\eta$ is measured between leptons, and M, p_T are the invariant mass and transverse momentum of the lepton pair.

The measured cross-sections as a function of y_Z are in agreement with NNLO predictions using different PDF sets. None of the generators show particularly good agreement with the data as a function of ϕ^*.

6 Z+b-jet

The analysis builds on the Z + jet result (JHEP01 (2014) 033). Jets are formed using particle flow with the anti-k_T algorithm and the b-tagging efficiency is taken from simulation.

A selection that forms displaced vertices is used to enrich the sample with b-jets. The b-jet yield is extracted from a $\mathcal{L}$-fit to the corrected mass, where M_{corr} is defined as

$$M_{corr} \equiv \sqrt{M^2 + p^2 \sin^2\theta} + p\sin\theta,$$

where M and p are the invariant mass and momentum of all tracks in the jet that are inconsistent with originating directly from the pp collision. The angle θ is between the momentum and the direction from the pp collision to the displaced vertex. Templates for b, c, and l-jets are taken from simulation.

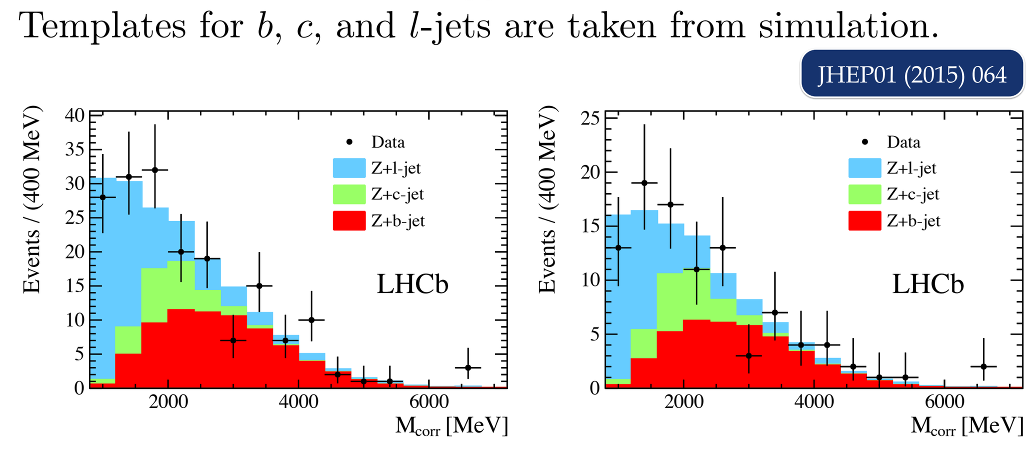

M_{corr} distribution for $p_T^{jet} > 10$ GeV (left) and $p_T^{jet} > 20$ GeV (right). Data (black points) are compared to the template fit results. The uncertainties shown are statistical only.

$\sigma_{Z\rightarrow\mu^+\mu^-+b-jet}$ cross-section at 7 TeV for $p_T^{jet} > 10$ GeV,

$$\sigma(Z + b - jet) = 295 \pm 60\,(stat.) \pm 51\,(syst.) \pm 10\,(lumi.)\text{fb}$$

for $p_T^{jet} > 20$ GeV,

$$\sigma(Z + b - jet) = 128 \pm 36\,(stat.) \pm 22\,(syst.) \pm 5\,(lumi.)\text{pb}$$

Results are compared to a theory prediction at LO and NLO with a correction for showering and hadronisation.

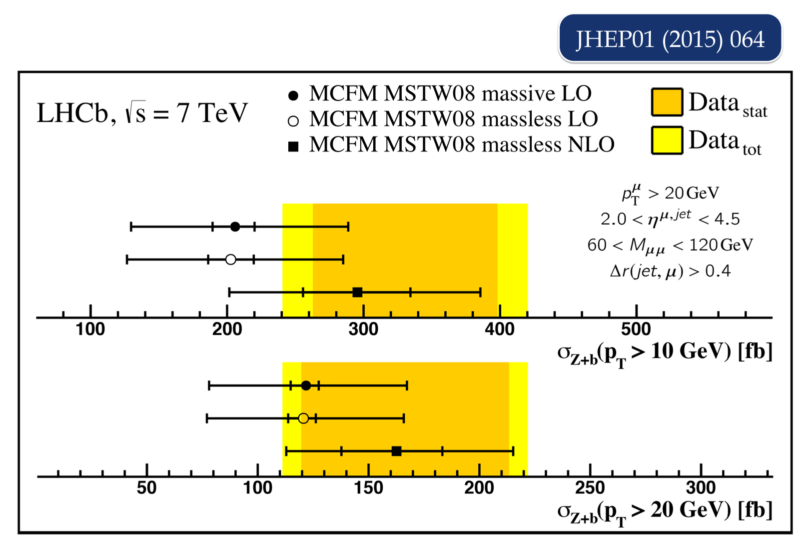

Inclusive cross-sections for $p_T^{jet} > 10$ GeV (above) and $p_T^{jet} > 20$ GeV (below) compared to MCFM with PDF and scale uncertainties. MCFM has been corrected for showering and hadronisation.

7 Conclusion

Three new results in electroweak physics from LHCb are presented. The W cross-section at 7 TeV is measured in the muon final state, an update to the Z $\rightarrow$ e$^+$e$^-$ is presented at an increased centre-of-mass energy of 8 TeV, and Z+b-jet production is studied at 7 TeV. The measurements are generally found to be in agreement with theory predictions and different NNLO PDF sets are contrasted.

LHCb is continuing to build on past successes in its electroweak program and is successfully branching into jet physics. Measurements made at LHCb are seen to have an impact on PDFs and the higher energies of Run II will extend our reach to yet lower values of x.